https://doi.org/10.5194/egusphere-2026-142
Preprint. Discussion started: 28 January 2026

Phenology-modulated Crop Responses to the 2024 Spring-Early Summer Compound Dry-Hot Event in the North China Plain

Linying Ma[1,2], Jun Wang[1,2,*], Zishan Wang[1,2], Qian Zhang[3,*], Ran Yan[3], Zhi Huang[1,2], Yabin Ye[1,2], Hao Zheng[1,2], Shuyue Xiao[1,2], Xiaokang Zhang[3], Zhenhai Li[3], Hongzhang Wang[4], Tao Wei[5], Haijin Dai[6], Meirong Wang[7], Xiuying Zhang[1,2]

[1] International Institute for Earth System Science, Nanjing University, Nanjing, Jiangsu 210023, China
[2] Jiangsu Provincial Key Laboratory of Geographic Information Science and Technology, Key Laboratory for Land Satellite Remote Sensing Applications of Ministry of Natural Resources, School of Geography and Ocean Science, Nanjing University, Nanjing, Jiangsu 210023, China
[3] College of Geodesy and Geomatics, Shandong University of Science and Technology, Qingdao 266590, China
[4] College of Agronomy, Shandong Agricultural University, Tai'an, Shandong 271018, China
[5] MountTai Management Committee, Tai'an, Shandong 271000, China
[6] College of Meteorology and Oceanography, National University of Defense Technology, Changsha, China
[7] State Key Laboratory of Climate System Prediction and Risk Management, Key Laboratory of Meteorological Disaster, Ministry of Education, Collaborative Innovation Center on Forecast and Evaluation of Meteorological Disasters, Nanjing University of Information Science and Technology, Nanjing, China

**Correspondence to*: Jun Wang (wangjun@nju.edu.cn); Qian Zhang (skd994880@sdust.edu.cn)

Abstract. Compound dry-hot events are intensifying under climate change and pose growing risks to agricultural production. From April to June 2024, the North China Plain (NCP) experienced an extreme compound dry-hot event. Using satellite-based normalized difference vegetation index (NDVI), gross primary productivity (GPP), and crop yield statistics, this study quantified crop growth responses and identified the dominant climatic drivers during this event. The climate anomaly was characterized by pronounced warming in April and June, a continuous decline in precipitation and soil water from April onward, and a record-high vapor pressure deficit (VPD) in June, forming a persistent dry-hot stress. NDVI

https://doi.org/10.5194/egusphere-2026-142
Preprint. Discussion started: 28 January 2026

and GPP increased markedly in April and remained slightly positive in May, but both collapsed to their lowest levels since 2000 in June. Consistent with these vegetation signals, provincial yield statistics and experimental plot observations showed increased winter wheat yields but reduced summer maize yields. Sensitivity and contribution analyses revealed distinct phenology-modulated mechanisms: in April, elevated temperatures and vegetation carryover effects comparably enhanced vegetation activity in winter-wheat-dominated croplands; in May, vegetation dynamics were controlled almost entirely by the previous-month carryover effect, reflecting the growing influence of accumulated vegetation state; and in June, as winter wheat reached maturity and newly sown maize entered early establishment, VPD emerged as the primary limiting factor, strongly suppressing photosynthetic activity and seedling establishment. These findings demonstrate how phenological transitions modulate crop vulnerability to compound dry-hot events and provide useful insights for agricultural early warning, crop management, and climate adaptation strategies in the NCP.

Keywords: Compound dry-hot events, normalized difference vegetation index (NDVI), gross primary productivity (GPP), Crop phenology, North China Plain

1 Introduction

Climate change accounts for nearly one-third of global crop yield fluctuations (Ray et al., 2015), underscoring the crucial role of climate conditions in sustaining agricultural productivity. As global warming accelerates, the frequency and intensity of weather and climate extremes have increased, surpassing previous records (Fischer et al., 2025). Events, such as droughts and heatwaves, are projected to become more frequent and severe in the future (AghaKouchak et al., 2020). These extremes substantially reduce crop growth and yields, further destabilizing global food markets and driving price volatility (Mehrabi and Ramankutty 2019; Tigchelaar et al., 2018; Vogel et al., 2019).

Globally, heatwaves have been found to reduce maize and wheat yields by 12.4% and 4.1%, respectively, while droughts cause declines of about 7% (Jägermeyr and Frieler 2018). In Europe, the 2003 drought and heatwave resulted in a 10% reduction in total crop production, including decreases of 11% for wheat and 21% for maize (García-Herrera et al., 2010). However, crop sensitivity to climate varies considerably across regions. For instance, wheat yields in western North America, eastern China, and

https://doi.org/10.5194/egusphere-2026-142
Preprint. Discussion started: 28 January 2026

Europe are highly sensitive to climatic fluctuations, as are maize yields in North America and China, whereas wheat in northern India and Pakistan exhibits weaker sensitivity (Heino et al., 2023).

Although temperature-related indicators generally show stronger associations with crop yields than precipitation-related ones (Lobell et al., 2011; Vogel et al., 2019), other climatic factors within the same growth season can also play substantial roles. Moreover, crop responses to climate anomalies often differ across phenological stages (Kaur and Behl 2010). Yet, it remains unclear which climate factors dominate crop growth at different stages under extreme conditions—an issue that warrants further investigation.

The rapid advancement of remote sensing technology now enables continuous monitoring of crop growth and its responses to climate variability at various multiple spatial and temporal scales (Huete 2016). Among remote-sensing-based vegetation indicators, the Normalized Difference Vegetation Index (NDVI) has been widely applied to detect vegetation trends and assess climatic drivers (Chu et al., 2019; Gao et al., 2022; Wei et al., 2022). NDVI has also been used to predict crop yield indicators (Magney et al., 2016) and estimate yield statistical models (Satir and Berberoglu 2016). Gross primary productivity (GPP), in contrast, more directly reflects ecosystem photosynthetic activity and responds rapidly to climatic extremes (Deng et al., 2021). As a key metric for evaluating farmland carbon budgets and crop growth conditions (Peng and Gitelson 2012), GPP complements NDVI in capturing vegetation dynamics under environmental stress. Together, these two indices provide robust tools for quantifying crop responses to climate change.

The North China Plain (NCP) is one of China's most vital grain-producing regions, exerting significant influence on national food security. However, this region has faced increasing exposure to extreme weather events—including heatwaves, droughts, heavy rainfall, and floods—that have posed mounting challenges to agricultural stability (Ding et al., 2025; Yu et al., 2016; Zhang et al., 2025). Precipitation across the NCP has declined since the mid-to-late 1970s, accompanied by a shift toward warmer and drier conditions that threaten crop production (Ma 2007). From April to June 2024, the NCP experienced moderate to severe drought conditions (Zhang et al., 2025), severely affecting crop growth during a critical stage of the growing season. This study aims to: (1) identify the spatiotemporal relationship between the 2024 spring-early summer climate anomaly and crop responses in the NCP; (2) analyze the sensitivity of NDVI and GPP to different climate factors from April to June; and (3) quantify the contributions of various climate drivers to abnormal changes in NDVI and GPP. By addressing these

https://doi.org/10.5194/egusphere-2026-142
Preprint. Discussion started: 28 January 2026

objectives, this study enhances understanding of crop response mechanisms under extreme climatic conditions and provides a scientific foundation for improving regional agricultural risk management and climate adaptation strategies.

2 Data and Methods

2.1 Study area

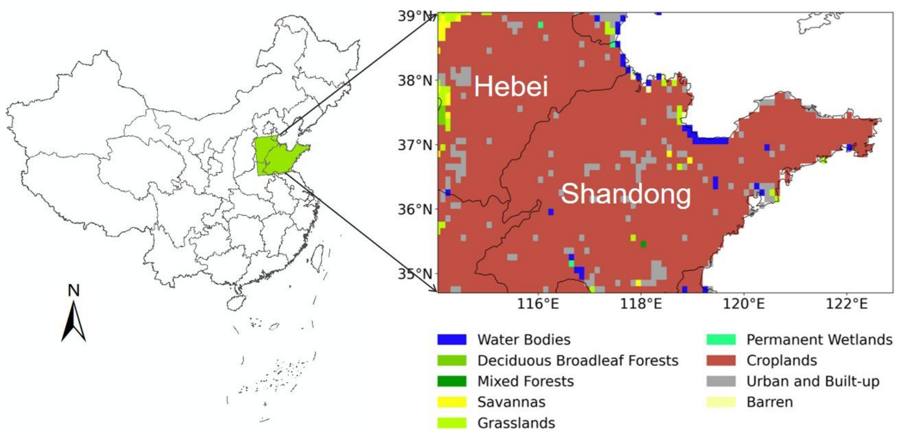

Figure 1. Geographic location and land use distribution of the study area, derived from the MODIS MCD12C1 land cover product.

The study area is located in the NCP, characterized by a temperate monsoon climate with noticeable seasonal fluctuations. Annual precipitation is predominantly concentrated between June and August and exhibits considerable interannual variability. Land cover data were obtained from the 2023 MODIS MCD12C1 version 6.1 product from the Terra and Aqua satellites at a spatial resolution of 0.05°×0.05°. Based on the International Geosphere-Biosphere Programme (IGBP) classification system, the region is mainly composed of croplands (Fig. 1). To focus on agricultural response processes, non-cropland grids were masked. Agricultural production in the NCP primarily relies on a double-cropping rotation system, with winter wheat sown in October and harvested in June; summer maize sown in June and harvested in September as the primary crops—both highly sensitive to climatic anomalies (Ling et al., 2023; Tao and Zhang 2010; Wang et al., 2019). According to the China Statistical Yearbook, Shandong and Hebei

https://doi.org/10.5194/egusphere-2026-142
Preprint. Discussion started: 28 January 2026

provinces together produced approximately 30% of the nation's total wheat and 16% of its maize in 2023, underscoring its importance as a key grain-producing region. This study focused on a region within the NCP where the 2024 climatic anomalies were particularly pronounced, to better assess crop responses.

2.2 Data sources

2.2.1 Climate Data

The climate data were obtained from the ERA5-Land monthly reanalysis dataset, spanning the period 2000-2024 with a spatial resolution of 0.1°×0.1° (Muñoz Sabater 2019). The primary variables include 2 m dewpoint temperature (TD), 2 m air temperature (TAS), volumetric soil water (SW), total precipitation (PRE), and surface solar radiation downwards (SSRD). ERA5-land, developed by the European Centre for Medium-Range Weather Forecasts (ECMWF), represents the fifth-generation global land reanalysis product. Building upon the ERA5 atmospheric reanalysis, in integrates an improved land surface model and higher-resolution grid design, providing enhanced representations of land surface energy and water balance processes.

The SW is provided for four soil layers (0-7 cm, 7-28 cm, 28-100 cm, and 100-289 cm). Following Wang et al. (2025a), we calculated the depth-weighted mean soil water content for the upper 100 cm, based on the first three layers.

Additionally, vapor pressure deficit (VPD) was derived from TAS and TD using Eq. (1) (Wang et al., 2023b):

$$\mathrm{VPD}=0.61078\times\left(e^{\frac{17.27\times \mathrm{TAS}}{\mathrm{TAS}+237.29}}-e^{\frac{17.27\times \mathrm{TD}}{\mathrm{TD}+237.29}}\right) \tag{1}$$

where TAS and TD are expressed in degrees Celsius, and VPD is measured in kilopascals (kPa). Given the monthly VPD anomalies derived from daily and monthly ERA5 data are nearly identical (He et al., 2022), we directly computed VPD using the monthly TAS and TD values in this study.

2.2.2 Vegetation and Crop Yield Data

The NDVI data were obtained from the MODIS MOD13C1 monthly product from the Terra satellite, covering the period from 2000 to 2024 with a spatial resolution of 0.05°×0.05°. GPP data were sourced from the FluxSat GPP v2.2 product, which provides daily estimates at the same spatial resolution and temporal coverage. The daily GPP data were aggregated to monthly values for comparison with NDVI. The

https://doi.org/10.5194/egusphere-2026-142
Preprint. Discussion started: 28 January 2026

FluxSat GPP dataset integrates geometrically corrected MODIS reflectance data with eddy covariance flux measurements from the FLUXNET 2015 network. It employs a simplified light-use efficiency (LUE) framework combined with neural network algorithms to estimate GPP at high spatiotemporal resolution (Joiner et al., 2018). To ensure spatial consistency across datasets, both NDVI and GPP were resampled to 0.1°×0.1° to match the climate data.

We also compiled province-level annual yields of winter wheat and summer maize for 2020-2024 from the China Statistical Yearbook. In addition, we used observed yields of winter wheat (varieties Shimai and Jimai) from 2023 to 2025 and summer maize (varieties Lainong14 and Zhengdan958) from 2022 to 2024 at an experimental plot (lat/long: 36.1565°N/117.1607°E). Each variety was grown in two to three replicated trials under a conventional fertilization regime, and all measurements were conducted by the same operator to ensure consistency in procedures and standards. Detailed yield information for all varieties is provided in Table S1 and S2.

2.3 Statistical methods

2.3.1 Anomaly Calculation

Anomalies were defined as the deviation of a variable from its long-term mean for the corresponding month. Using 2001-2023 as the reference period, monthly anomalies of climatic variables and vegetation indices were calculated for 2000-2024. To minimize the influence of long-term CO_2 fertilization and climate warming on vegetation dynamics, a linear detrended procedure was applied to each variable through ordinary least squares regression. The resulting detrended anomalies were used in subsequent analyses.

For the province-level statistics of winter wheat and summer maize yields, we quantified their relative changes (RC) using Eq. (2):

$$RC = \frac{Yield_{2024} - Yield_{mean}}{Yield_{mean}} \times 100\% \quad (2)$$

where $Yield_{2024}$ and $Yield_{mean}$ denote the yield of winter wheat/summer maize in 2024 and the average yield over 2020-2024 (kg hm^{-2}), respectively. RC is expressed as a percentage (%).

2.3.2 Multiple Linear Regression Model

https://doi.org/10.5194/egusphere-2026-142
Preprint. Discussion started: 28 January 2026

To investigate the sensitivity and relative contributions of climatic factors on NDVI and GPP anomalies, we applied a multiple linear regression (MLR) analysis for the period March-June during 2000-2024 which was widely used by previous studies (Wang et al., 2023a; Wang et al., 2023b; Wang et al., 2026). The independent variables included TAS, VPD, PRE, SW, SSRD, and the lagged NDVI (or GPP) anomaly from the previous month. The general form of the model uses Eq. (3):

$$Y_t=\beta_1 TAS_t+\beta_2 VPD_t+\beta_3 SW_t+\beta_4 PRE_t+\beta_5 SSRD_t+\beta_6 Y_{t-1}+\varepsilon \quad (3)$$

where Y_t is the NDVI (or GPP) anomaly in month t (GPP in gC m^{-2} mo^{-1}), and Y_{t-1} is the anomaly value for previous month. TAS_t, VPD_t , SW_t, PRE_t and $SSRD_t$ denote the anomalies of near-surface air temperature (°C), vapor pressure deficit (kPa), soil water (m^3 m^{-3}), total precipitation (mm mo^{-}1), and downward shortwave radiation (W m^{-2}), respectively. β_i represents the regression coefficients, and ε is the residual term. The overall model performance was assessed using the F-test and the coefficient of determination (R^2). A p-value < 0.05 was taken as the threshold for statistical significance, and the significance of individual predictors was evaluated using t-test.

To eliminate the influence of differing variable units, standardized regression coefficients were used to measure the relative sensitivity of NDVI and GPP to each climatic factor. These coefficients were obtained by performing regression on standardized variables, enabling direct comparability across predictors.

To quantify the magnitude of each factor's contribution to the observed NDVI or GPP anomaly, we calculated monthly contributions using Eq. (4):

$$Contribution_{i,t} = \beta_{i,t} \times X_{i,t} \quad (4)$$

where $Contribution_{i,t}$ is the contribution of variable i in month t, $\beta_{i,t}$ is the regression coefficient of variable i in month t in the multiple linear regression model, and $X_{i,t}$ is the corresponding detrended anomaly.

3 Results

3.1 April-June 2024 Compound Dry-Hot Event

https://doi.org/10.5194/egusphere-2026-142
Preprint. Discussion started: 28 January 2026

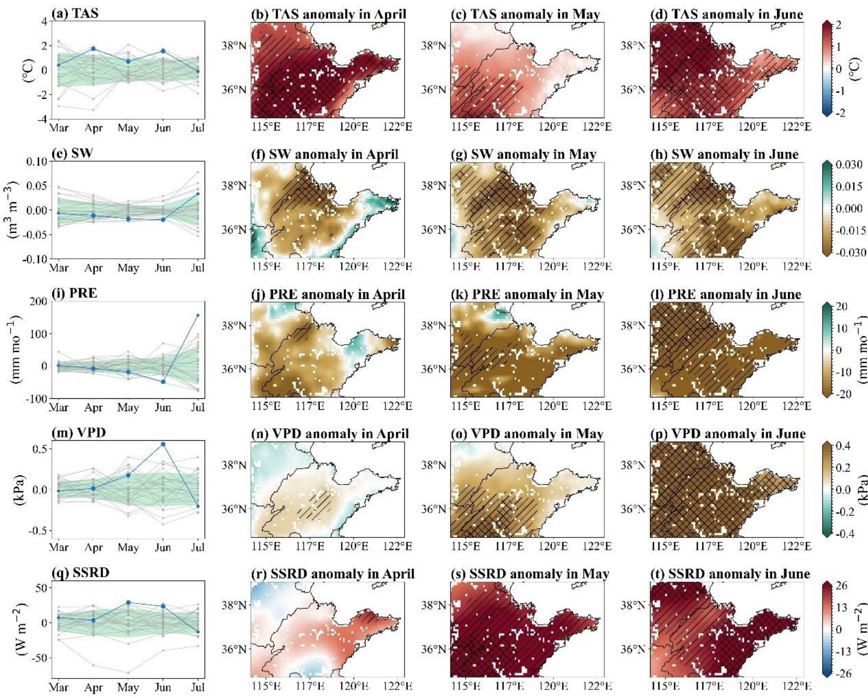

Figure 2. Detrended climate anomalies over the NCP from March to July, including (a) near-surface air temperature (TAS), (e) soil water (SW), (i) precipitation (PRE), (m) vapor pressure deficit (VPD), and (q) surface shortwave radiation downward (SSRD). The blue lines denote the anomalies for 2024, while the green shaded areas indicate the interannual variability represented by one standard deviation (1σ) during 2000-2023. Panels (b-d), (f-h), (j-l), (n-p), and (r-t) show the spatial distributions of TAS (℃), SW ($m^3\ m^{-3}$), PRE ($mm\ mo^{-1}$), VPD (kPa), and SSRD ($W\ m^{-2}$) anomalies, respectively, from April to June 2024. Areas marked with "//" indicate anomalies exceeding 1σ, while those labeled "XX" exceed 1.5σ.

In 2024, we find that significantly higher temperatures occurred in April and June over the NCP, far exceeding the historical interannual variability represented by one standard deviation (1σ) (Fig. 2a). During these months, precipitation continuously decreased, reaching the lowest in June 2024 (Fig. 2i). Hence, associated with enhanced evapotranspiration, soil water content continued to decline before July, with the anomalous values exceeding the historical interannual variability in May and June, exhibiting extreme

https://doi.org/10.5194/egusphere-2026-142
Preprint. Discussion started: 28 January 2026

droughts (Fig. 2e). Simultaneously, reduced atmospheric actual water vapor induced by the continuous decline in precipitation and enhanced saturated water vapor induced by higher temperatures lead to the continuous increase in VPD, showing the record-breaking atmospheric dryness in June 2024 (Fig. 2m). Additionally, associated with this compound dry-hot event, SSRD showed significant increase in May and June (Fig. 2q).

Spatially, April exhibited markedly higher temperatures (>1.5σ) across nearly the entire Shandong province (Fig. 2b), accompanied by severe droughts (below −1.5σ) in the northeastern Shandong (Fig. 2d). In May, precipitation further declined in the central and western regions (Fig. 2k), while areas of notably low soil water expanded southward (Fig. 2g). Although the temperature anomalies weakened, VPD began to increase in the southern areas, indicating obvious atmospheric dryness (Fig. 2o). SSRD also rose substantially due to reduced cloud cover (Fig. 2s). By June, the entire region again experienced intense warming, with TAS anomalies exceeding 1.5σ, while precipitation reached its lowest levels (Figs. 2d and 2l). Under the combined effects of heat and persistent rainfall deficit, soil water depleted further, VPD reached record highs, and SSRD remained elevated across almost all areas (Figs. 2h, 2p, and 2t).

3.2 Influence on crop growth and yields

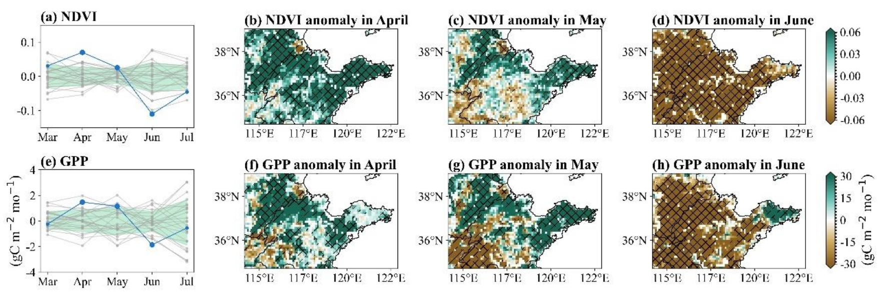

Figure 3. Detrended vegetation index anomalies over the NCP from March to July, including (a) the normalized difference vegetation index (NDVI) and (e) FluxSat gross primary production (GPP). The blue lines denote vegetation index anomalies for 2024, while the green shaded areas represent interannual variability presented by one standard deviation (1σ) during 2000-2023. Panels (b-d) and (f-h) show the spatial distributions of NDVI and GPP (gC m^{-2} mo^{-1}) anomalies, respectively, from April to June 2024. Areas marked with "//" indicate anomalies exceeding 1σ, while those labeled "XX" exceed 1.5σ.

https://doi.org/10.5194/egusphere-2026-142
Preprint. Discussion started: 28 January 2026

We find that NDVI in April 2024 exceeded 1.5σ, reaching its highest value since 2000 (Fig. 3a), while GPP also showed a marked increase (Fig. 3e). These results indicate that elevated temperatures in April substantially enhanced crop growth, overweighing the modest inhibitory effects of mild dryness. Spatially, both NDVI and GPP anomalies were strongly positive across most of the NCP, except in the southwest (Figs. 3b and 3f).

In May, temperatures moderated, but drought intensity increased and VPD began to rise (Fig. 2). Although NDVI and GPP decreased notably in the southwest, most regions still exhibited positive anomalies (Figs. 3c and 3g), leading to a slight but overall positive regional mean (Figs. 3a and 3e). Despite enhanced soil and atmospheric dryness, NDVI and GPP did not show a pronounced decline.

By June, extreme compound heat and drought conditions dominated the NCP (Figs. 2d, 2h and 2p), driving both NDVI and GPP to record lows (Figs. 3a and 3e). Except for a few eastern areas, nearly the entire region exhibited significant decreases in NDVI and GPP, with anomalies falling below −1.5σ (Figs. 3d and 3h). Notably, vegetation responses during June were further complicated by regional cropping practices: winter wheat is typically harvested in early June (Luo et al., 2020), after which maize is sown. The combination of heat and drought conditions likely hindered maize establishment-conditions that can impair germination, suppress early growth, and reduce canopy development-thereby amplifying reductions in NDVI and GPP.

https://doi.org/10.5194/egusphere-2026-142
Preprint. Discussion started: 28 January 2026

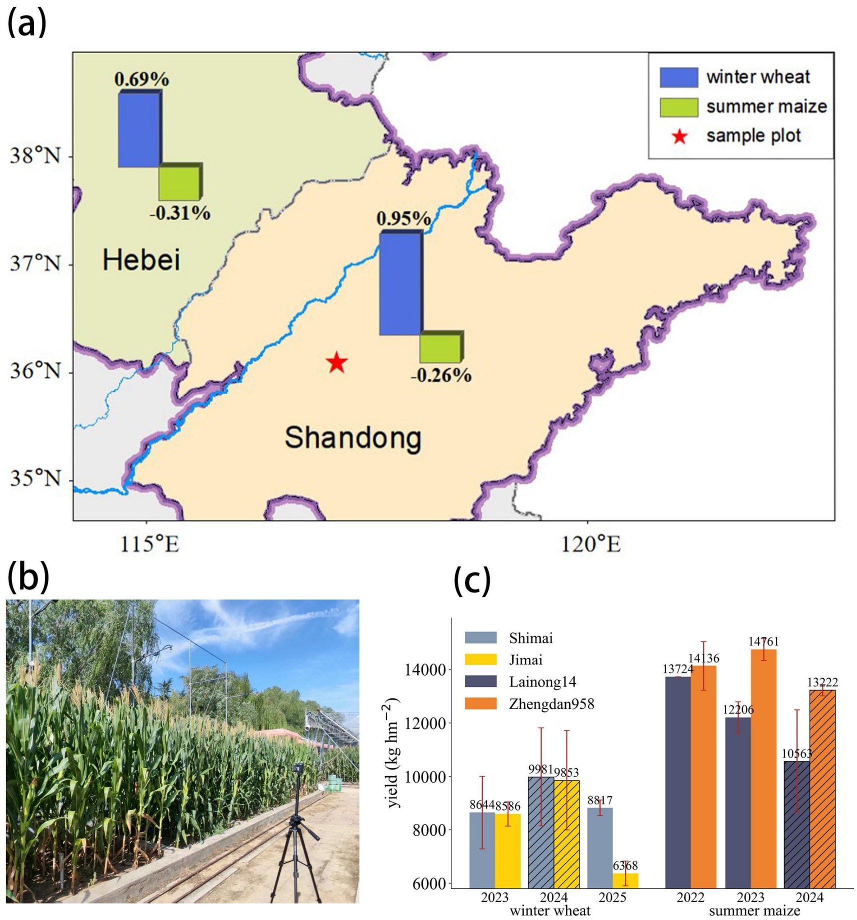

Figure 4. Annual yield changes of winter wheat and summer maize. (a) Relative changes (RC) in 2024 winter wheat and summer maize yields across key provinces in the study area. The asterisk marks the sample plot located in Shandong province. (b) Field photographs of the sample site. (c) Observed yields of winter wheat (varieties Shimai and Jimai) for 2023-2025 and summer maize (varieties Lainong14 and Zhengdan958) for 2022-2024 at the plot.

The climatic conditions in spring can strongly influence tillering, young ear development, and grain filling in winter wheat (He et al., 2020; Li et al., 2015; Xiao et al., 2018), thereby shaping its final yield. In

https://doi.org/10.5194/egusphere-2026-142
Preprint. Discussion started: 28 January 2026

the study area, early-summer climate also affects maize emergence and seedling vigor (Lin et al., 2015; Wang et al., 2022), with potential impacts on annual summer maize production. Therefore, using annual winter wheat and summer maize yield statistics from the National Bureau of Statistics, we compute their relative changes in 2024 to assess the potential impacts of this compound dry-hot event. Province-level yield data indicate slight enhancements in winter wheat production (0.69% in Hebei and 0.95% in Shandong) and reductions in summer maize yield (-0.31% in Hebei and -0.26% in Shandong) in 2024 (Fig. 4a), broadly consistent with the NDVI and GPP anomalies (Fig. 3). Observations from the sample plot also show that, for the same varieties, winter wheat yields increased while maize yields declined relative to adjacent years (Fig. 4c). Quantitatively, year-on-year increases in winter wheat reached 15% for both Shimai and Jimai in 2024, whereas summer maize yields decreased by 13% for Lainong14 and 10% for Zhengdan958.

3.3 Sensitivities of Crop Growth to Different Driving Factors

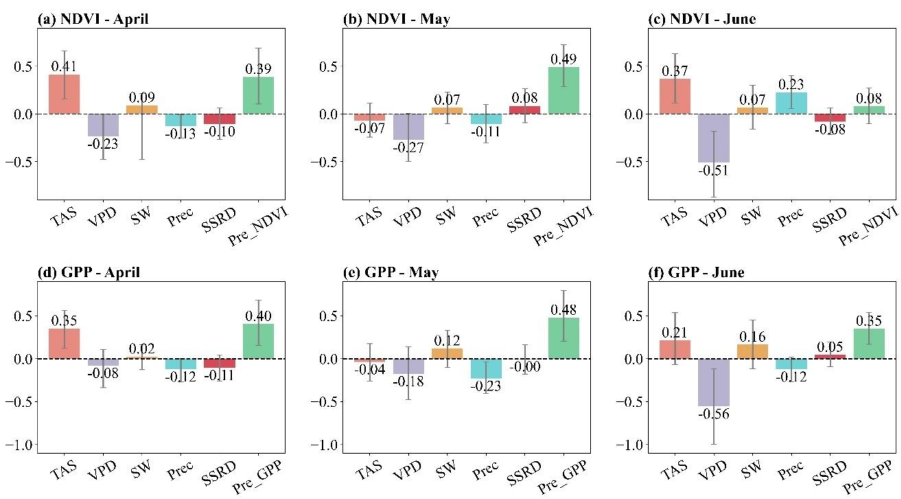

Figure 5. Standardized sensitivities of (a-c) NDVI and (d-f) GPP anomalies to multiple driving factors from April to June over the NCP. The driving factors include TAS, VPD, SW, PRE, SSRD, and the previous month's NDVI or GPP (Pre_NDVI or Pre_GPP).

https://doi.org/10.5194/egusphere-2026-142
Preprint. Discussion started: 28 January 2026

To quantify how crop responses to various environmental drivers, we examined the standardized regression coefficients of NDVI and GPP against multiple factors. In April, both NDVI and GPP exhibited strong positive sensitivities to TAS, with coefficients of 0.42 and 0.35, respectively. They also showed comparable sensitivities to vegetation conditions in the previous month (Pre_NDVI or Pre_GPP; 0.39 and 0.40, respectively), suggesting that concurrent higher temperatures and vegetation carryover effects could jointly enhance crop growth during this period (Figs. 5a and 5d). Sensitivities to other climatic factors were relatively weak.

In May, as temperatures moderated and dryness began to increase, sensitivities of NDVI and GPP to most climate factors showed relatively weak, though VPD sensitivities increased slightly (Figs. 5b and 5e). Both NDVI and GPP showed significant positive sensitivities to previous-month vegetation conditions (0.49 and 0.48, respectively), indicating that the continued positive anomalies in May were primarily due to the vegetation carryover effect.

By June, when compound heat and drought extremes prevailed (Fig. 2), associated with the transition in cropping practices, both NDVI and GPP exhibited their strongest negative sensitivities to VPD (-0.51 and -0.56, respectively), while maintaining positive responses to higher temperatures. Notably, GPP still showed a substantial positive sensitivity to previous-month vegetation conditions (0.35), even stronger than its sensitivity to TAS, whereas NDVI displayed no significant dependence on previous-month conditions (Figs. 5c and 5f).

Spatially, NDVI and GPP exhibited positive sensitivity to TAS across most regions in April and June, with particularly strong responses in eastern regions during April (Figs. S1a, S1c, S2a, and S2c). Sensitivity to previous-month conditions was also pronounced in April and further expanded in May (Figs. S1p, S1q, S2p, and S2q). In June, positive sensitivity to SW intensified in the east, whereas negative sensitivity to VPD strengthened across nearly the entire NCP (Figs. S1f, S1l, S2f, and S2l).

3.4 Individual Contributions of Different Driving Factors

https://doi.org/10.5194/egusphere-2026-142
Preprint. Discussion started: 28 January 2026

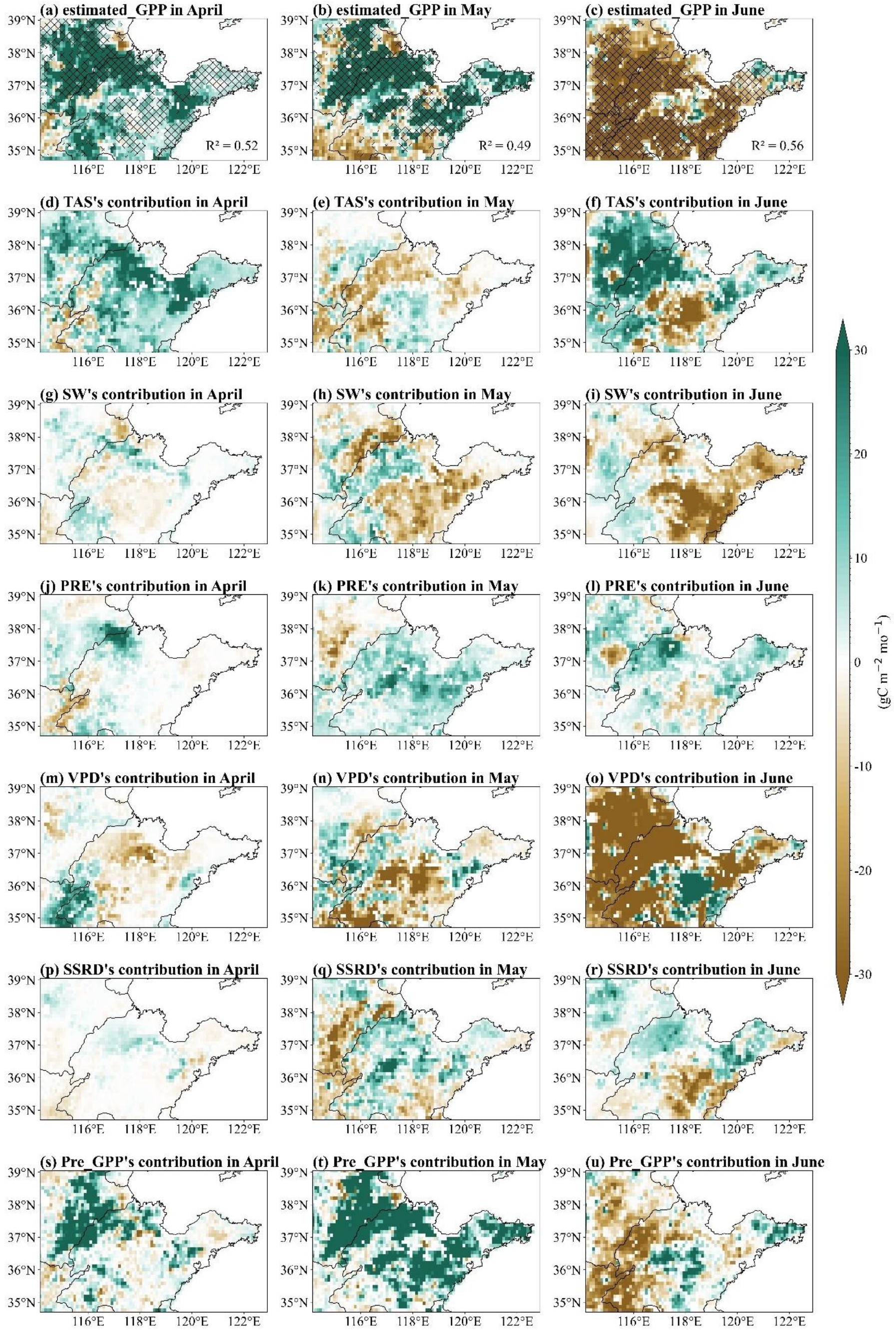

287

https://doi.org/10.5194/egusphere-2026-142
Preprint. Discussion started: 28 January 2026

Figure 6. Geographical distributions of individual contributions from different driving factors. (a-c) Estimated GPP during April-June 2024 based on the multiple linear regression model. Shaded areas labeled "XX" indicate grid cells where the model's F-test p-value is < 0.05. Panels (d-f), (g-i), (j-l), (m-o), (p-r), and (s-u) present the separated contributions from TAS, SW, PRE, VPD, SSRD, and Pre_GPP, respectively.

Beyond sensitivity analysis, we further quantified the pixel-level contributions of individual drivers to NDVI and GPP anomalies during April-June 2024. Because NDVI and GPP exhibited broadly consistent responses, and GPP variations are more directly linked to crop production, we focus on the spatial patterns of contributions to GPP in Figure 6, while the corresponding NDVI results are provided in supplementary Figure 3. The MLR model reproduced GPP anomalies well, with widespread statistical significance ($p < 0.05$) and R^2 of ~0.6 (Figs. 6a-c), consistent with the observed anomalies (Figs. 3f-h).

In April, enhanced GPP over northern regions was primarily attributable to positive effects from TAS and Pre_GPP, aligning with their strong sensitivities, although their areas of influence differed (Figs. 6a, 6d, and 6s). In May, the persistence of high GPP in the northern and eastern areas was dominated by Pre_GPP contributions (Fig. 6t), whereas reductions in southwestern regions were mainly driven by VPD (Fig. 6n). By June, widespread GPP declines were largely linked to strong VPD inhibition (Fig. 6o), consistent with the strongest negative standardized sensitivity (−0.56; Fig. 5f). Additional reductions over the southeastern areas arose from combined effects of high TAS and soil droughts (Figs. 6f and 6i). Although Pre_GPP remained a statistically meaningful predictor, its June contribution was relatively weak, despite its high sensitivity (Figs. 5f and 6u). Notably, positive TAS effects mitigated part of the VPD-induced decline in northern areas (Fig. 6f).

https://doi.org/10.5194/egusphere-2026-142
Preprint. Discussion started: 28 January 2026

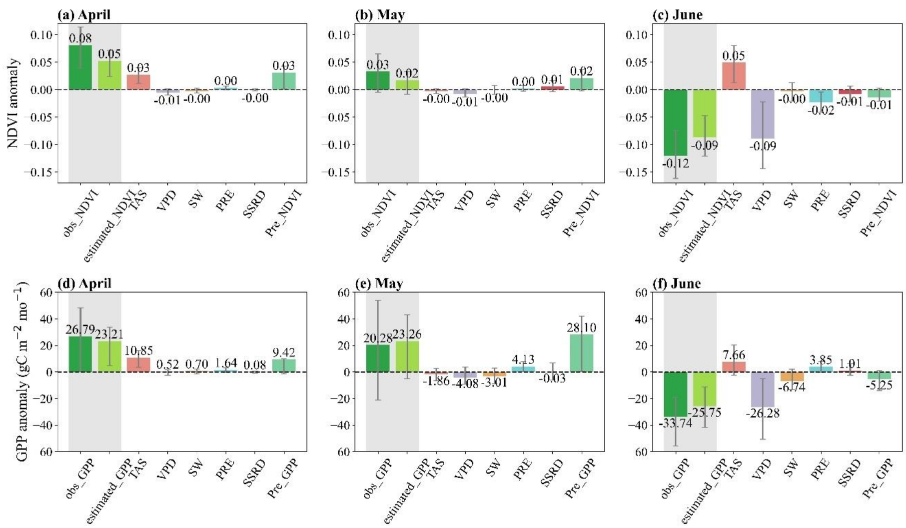

Figure 7. Contributions of individual driving factors to regional mean (a-c) NDVI and (d-f) GPP anomalies during April-June 2024. The explanatory variables include TAS, VPD, SW, PRE, SSRD, and the previous-month vegetation conditions (Pre_NDVI or Pre_GPP). Each panel also displays the estimated anomalies (estimated_NDVI or estimated_GPP) and observed anomalies (obs_NDVI or obs_GPP).

To quantify these contributions regionally, Figure 7 compares estimated and observed NDVI and GPP anomalies, demonstrating good agreement and supporting model robustness. In April, TAS and previous-month vegetation conditions contributed comparably (both 0.03 for NDVI; 10.86 and 9.42 gC m^{-2} mo^{-1} for GPP). In May, nearly all positive anomalies were attributable to Pre_NDVI (0.02) and Pre_GPP (28.11 gC m^{-2} mo^{-1}). By June, VPD became the dominant suppressing factor, contributing −0.09 to NDVI and −26.30 gC m^{-2} mo^{-1} to GPP. Consistent with spatial patterns, TAS partially offset this inhibition, contributing 0.05 to NDVI and 7.67 gC m^{-2} mo^{-1} to GPP.

4 Discussion

4.1 Mechanistic Differences in Crop response to Compound Dry-Hot Events

The impacts of compound dry-hot events on crop yields remain insufficiently understood (Feng et al., 2019; Heino et al., 2023). This study investigated the rapid responses of major crops to the 2024 compound

https://doi.org/10.5194/egusphere-2026-142
Preprint. Discussion started: 28 January 2026

dry-hot event, a process further complicated by regional cropping practices over the NCP. Through multiple linear regression analysis, we revealed that the dominant drivers of crop vulnerability shifted markedly across different months of the event.

In April, winter wheat in the booting-heading stage was highly temperature-responsive, with warming accelerating development and biomass accumulation (He et al., 2020; Wang et al., 2018). The strong contribution from the prior vegetation state also underscores the role of physiological memory effects (Wong et al., 2021; Zhou et al., 2020). By May, crop growth appeared more constrained by accumulated biomass than by concurrent weather variability, as evidenced by declining temperature sensitivity and a rising influence of antecedent vegetation (Fig. 5). This shift aligns with the understanding that after reproductive structures are formed, wheat productivity becomes primarily source-regulated rather than directly climate-driven (Ceglar et al., 2016). A sharp transition in dominant stressors occurred in June. Winter wheat approached maturity while maize entered germination. Elevated VPD increased atmospheric evaporative demand, inducing stomatal closure, restricting carbon assimilation, and ultimately reducing seedling vigor (Fu et al., 2022; Medrano et al., 2002; Schönbeck et al., 2022). Consequently, NDVI and GPP reached their lowest levels since 2000 (Fig. 3). The strong linkage between VPD and maize yield is consistent with evidence suggesting that, under dry-hot conditions, VPD may explain more yield variability than factors like fertilizer or irrigation (Rathore et al., 2024).

4.2 Agricultural Implications

These contrasting monthly sensitivities imply that a single compound event can simultaneously enhance winter wheat yield while suppressing maize yield, depending on crop phenology and water management. Consequently, adaptation requires stage-specific strategies. For maize during establishment, priorities should include conserving soil moisture and mitigating VPD impacts through practices such as mulching and timely irrigation. For winter wheat during reproductive growth may benefit from warming-induced acceleration where appropriate.

Under future global warming scenarios, compound dry-hot events are expected to become more frequent and intense, posing substantial threats to agricultural productivity and food security globally and in China (AghaKouchak et al., 2020; Heino et al., 2023; Mehrabi and Ramankutty 2019). As thermal and drought stresses intensify, maize yield losses across the NCP are likely to increase (Liu et al., 2025),

https://doi.org/10.5194/egusphere-2026-142
Preprint. Discussion started: 28 January 2026

although irrigation may partially offset these impacts (Wang et al., 2025b). Future efforts should focus on exploring adaptation options—such as optimizing sowing timing, varietal selection, and irrigation scheduling—within scenario analyses to identify robust strategies for increasing compound extremes. Concurrently, developing more heat-resistant and drought-resistant wheat and maize varieties will be essential.

4.3 Uncertainties and Limitations

Several caveats should be considered when generalizing these findings. The use of monthly vegetation and yield data may limit the detection of rapid phenological responses; higher-frequency monitoring would better capture establishment-phase stress dynamics. Crop production in the NCP heavily depends on groundwater extraction, and long-term overuse has led to severe aquifer depletion (Zhao et al., 2018), with winter wheat irrigation accounting for approximately 70% of total agricultural water use (Zhang et al., 2023). Our study did not explicitly represent irrigation or groundwater extraction processes, although these are critical for buffering climatic stress in this region. Furthermore, remote sensing-derived GPP estimates carry inherent uncertainties when applied to croplands (Gitelson et al., 2008; Zhang et al., 2014), necessitating future ground-truthing for validation.

5 Conclusions

This study systematically evaluated the impacts of the 2024 spring-early summer compound dry-hot event on major grain crops in the NCP. The key findings are as follows:

(1) The regional climate exhibited typical compound-extreme characteristics. April and June experienced pronounced warming, while precipitation and soil moisture declined persistently from April onward and approached record-low levels by June. Concurrently, VPD reached its highest value in the past two decades, indicating exceptionally strong atmospheric drought.

(2) Satellite-based vegetation indicators showed strong phenological and climatic imprints: NDVI and GPP increased markedly in April, remained slightly positive overall in May, but dropped to record lows in June. These variations were consistent with both province-level yield statistics and field-observed yields, which jointly indicate increased winter wheat yields but reduced summer maize yields.

(3) Sensitivity and contribution analyses revealed distinct stage-dependent drivers of crop physiological responses. In April, accelerated crop growth was primarily stimulated by elevated temperatures and strong vegetation carryover effects. In May, crop productivity became governed almost exclusively by previous-month vegetation conditions, underscoring the importance of physiological memory. By June—when winter wheat reached maturity and summer maize entered emergence—VPD became the dominant limiting factor, reflecting a sharp month-to-month shift in climatic controls.

Overall, this study demonstrates the rapid and phenology-dependent responses of crops in the NCP to compound dry-hot conditions. The results underscore the necessity of explicitly considering crop growth stages when assessing climate risks and identifying dominant stressors. These findings provide scientific support for agricultural disaster early warning, regional food-production management, and climate-adaptation policy development.

Author contribution

LM: Writing – original draft. JW: Writing – review & editing. ZW: Writing – review & editing. QZ: Writing – review & editing. RY: Writing – review & editing. ZH: Writing – review & editing. YY: Writing – review & editing. HZ: Writing – review & editing. SX: Writing – review & editing. XZ: Writing – review & editing. ZL: Writing – review & editing. HW: Writing – review & editing. HD: Writing – review & editing. TW: Writing – review & editing. MW: Writing – review & editing. XZ: Writing – review & editing.

Competing interests

The contact author has declared that none of the authors has any competing interests.

Acknowledgments

The calculations in this paper have been done on the computing facilities in the High Performance Computing Center (HPCC) of Nanjing University. This study was supported by the National Key Research and Development Program of China (grant no. 2023YFF0805401). This study was supported by the National Natural Science Foundation of China (Grants 42475129). QZ was supported by the Taishan Scholar project (tsqn202306210).

https://doi.org/10.5194/egusphere-2026-142
Preprint. Discussion started: 28 January 2026

Data Availability

FluxSat GPP Version 2.2 is available at https://disc.gsfc.nasa.gov/datasets/FluxSatMGPP_L3_Daily_p05deg_2.2/summary. The MODIS NDVI is provided at https://www.earthdata.nasa.gov/data/catalog/lpcloud-mod13c1-061. The MODIS land cover type data is available at https://www.earthdata.nasa.gov/data/catalog/lpcloud-mcd12c1-061. The yield data for wheat and maize is available at https://www.stats.gov.cn/sj/ndsj/. ERA5-Land is available at https://cds.climate.copernicus.eu/datasets/reanalysis-era5-land-monthly-means?tab=overview.

References

Aghakouchak, A., Chiang, F., Huning, L. S., Love, C. A., Mallakpour, I., Mazdiyasni, O., Moftakhari, H., Papalexiou, S. M., Ragno, E. and Sadegh, M.: Climate extremes and compound hazards in a warming world, Annu. Rev. Earth Planet. Sci., 48, 519–548, https://doi.org/10.1146/annurev-earth-071719-055228, 2020.

Ceglar, A., Toreti, A., Lecerf, R., Van Der Velde, M. and Dentener, F.: Impact of meteorological drivers on regional inter-annual crop yield variability in France, Agric. For. Meteorol., 216, 58–67, https://doi.org/DOI10.1016/j.agrformet.2015.10.004, 2016.

Chu, H., Venevsky, S., Wu, C. and Wang, M.: NDVI-based vegetation dynamics and its response to climate changes at Amur-Heilongjiang River Basin from 1982 to 2015, Sci. Total Environ., 650, 2051–2062, https://doi.org/DOI10.1016/j.scitotenv.2018.09.115, 2019.

Deng, Y., Wang, X., Wang, K., Ciais, P., Tang, S., Jin, L., Li, L. and Piao, S.: Responses of vegetation greenness and carbon cycle to extreme droughts in China, Agric. For. Meteorol., 298, 108307, https://doi.org/DOI10.1016/j.agrformet.2020.108307, 2021.

Ding, T., Xie, T., Gao, H. and Zhang, S.: Alternation Between the Extreme Drought-Flood Event in the North China Plain in Summer 2024, Int. J. Climatol., 45, e8831, https://doi.org/DOI10.1002/joc.8831, 2025.

https://doi.org/10.5194/egusphere-2026-142
Preprint. Discussion started: 28 January 2026

Feng, S., Hao, Z., Zhang, X. and Hao, F.: Probabilistic evaluation of the impact of compound dry-hot events on global maize yields, Sci. Total Environ., 689, 1228–1234, https://doi.org/DOI10.1016/j.scitotenv.2019.06.373, 2019.

Fischer, E. M., Bador, M., Huser, R., Kendon, E. J., Robinson, A. and Sippel, S.: Record-breaking extremes in a warming climate, Nat. Rev. Earth Environ., 6, 456–470, https://doi.org/10.1038/s43017-025-00681-y, 2025.

Fu, Z., Ciais, P., Prentice, I. C., Gentine, P., Makowski, D., Bastos, A., Luo, X., Green, J. K., Stoy, P. C. and Yang, H.: Atmospheric dryness reduces photosynthesis along a large range of soil water deficits, Nat. Commun., 13, 989, https://doi.org/10.1038/s41467-022-28652-7, 2022.

Gao, W., Zheng, C., Liu, X., Lu, Y., Chen, Y., Wei, Y. and Ma, Y.: NDVI-based vegetation dynamics and their responses to climate change and human activities from 1982 to 2020: A case study in the Mu Us Sandy Land, China, Ecol. Indic., 137, 108745, https://doi.org/10.1016/j.ecolind.2022.108745, 2022.

García-Herrera, R., Díaz, J., Trigo, R. M., Luterbacher, J. and Fischer, E. M.: A review of the European summer heat wave of 2003, Crit. Rev. Environ. Sci. Technol., 40, 267–306, https://doi.org/10.1080/10643380802238137, 2010.

Gitelson, A., Vina, A., Masek, J., Verma, S. and Suyker, A.: Synoptic monitoring of gross primary productivity of maize using Landsat data, IEEE Geosci. Remote Sens. Lett., 5, 133–137, https://doi.org/10.1109/lgrs.2008.915598, 2008.

He, B., Chen, C., Lin, S., Yuan, W., Chen, H. W., Chen, D., Zhang, Y., Guo, L., Zhao, X. and Liu, X.: Worldwide impacts of atmospheric vapor pressure deficit on the interannual variability of terrestrial carbon sinks, Natl. Sci. Rev., 9, nwab150, https://doi.org/10.1093/nsr/nwab150, 2022.

He, D., Fang, S., Liang, H., Wang, E. and Wu, D.: Contrasting yield responses of winter and spring wheat to temperature rise in China, Environ. Res. Lett., 15, 124038, https://doi.org/10.1088/1748-9326/abc71a, 2020.

Heino, M., Kinnunen, P., Anderson, W., Ray, D. K., Puma, M. J., Varis, O., Siebert, S. and Kummu, M.: Increased probability of hot and dry weather extremes during the growing season threatens global crop yields, Sci. Rep., 13, 3583, https://doi.org/10.1038/s41598-023-29378-2, 2023.

https://doi.org/10.5194/egusphere-2026-142
Preprint. Discussion started: 28 January 2026

Huete, A.: Vegetation's responses to climate variability, Nature, 531, 181–182, https://doi.org/10.1038/nature17301, 2016.

Jägermeyr, J. and Frieler, K.: Spatial variations in crop growing seasons pivotal to reproduce global fluctuations in maize and wheat yields, Sci. Adv., 4, 10, https://doi.org/10.1126/sciadv.aat4517, 2018.

Joiner, J., Yoshida, Y., Zhang, Y., Duveiller, G., Jung, M., Lyapustin, A., Wang, Y. and Tucker, C. J.: Estimation of terrestrial global gross primary production (GPP) with satellite data-driven models and eddy covariance flux data, Remote Sens., 10, 1346, https://doi.org/10.3390/rs10091346, 2018.

Kaur, V. and Behl, R.: Grain yield in wheat as affected by short periods of high temperature, drought and their interaction during pre-and post-anthesis stages, Cereal Res. Commun., 38, 514–520, https://doi.org/10.1556/CRC.38.2010.4.8, 2010.

Li, X., Cai, J., Liu, F., Dai, T., Cao, W. and Jiang, D.: Spring Freeze Effect on Wheat Yield is Modulated by Winter Temperature Fluctuations: Evidence from Meta-Analysis and Simulating Experiment, J. Agron. Crop Sci., 201, 288–300, https://doi.org/10.1111/jac.12115, 2015.

Lin, M., Xinjian, L., Dingrong, W. and Chunyi, W.: Responses of Summer Maize Main Phenology to Climate Change in the North China Plain, Chin. J. Agrometeorol., 36, 375–382, https://doi.org/10.3969/j.issn.1000-6362.2015.04.001, 2015.

Ling, M., Han, H., Hu, X., Xia, Q. and Guo, X.: Drought characteristics and causes during summer maize growth period on Huang-Huai-Hai Plain based on daily scale SPEI, Agric. Water Manag., 280, 108198, https://doi.org/10.1016/j.agwat.2023.108198, 2023.

Liu, Z., Qiu, R. and Zhang, Q.: Differences in effects of varying compound extreme temperature and precipitation events on summer maize yield in North China, Agric. Water Manag., 307, 109237, https://doi.org/10.1016/j.agwat.2024.109237, 2025.

Lobell, D. B., Schlenker, W. and Costa-Roberts, J.: Climate trends and global crop production since 1980, Science, 333, 616–620, 2011.

Luo, Y., Zhang, Z., Chen, Y., Li, Z. and Tao, F.: ChinaCropPhen1km: a high-resolution crop phenological dataset for three staple crops in China during 2000-2015 based on leaf area index (LAI) products, Earth Syst. Sci. Data, 12, 197–214, https://doi.org/10.5194/essd-12-197-2020, 2020.

https://doi.org/10.5194/egusphere-2026-142
Preprint. Discussion started: 28 January 2026

Ma, Z.: The interdecadal trend and shift of dry/wet over the central part of North China and their relationship to the Pacific Decadal Oscillation (PDO), Chin. Sci. Bull., 52, 2130–2139, https://doi.org/10.1007/s11434-007-0284-z, 2007.

Magney, T. S., Eitel, J. U., Huggins, D. R. and Vierling, L. A.: Proximal NDVI derived phenology improves in-season predictions of wheat quantity and quality, Agric. For. Meteorol., 217, 46–60, https://doi.org/10.1016/j.agrformet.2015.11.009, 2016.

Medrano, H., Escalona, J. M., Bota, J., Gulías, J. and Flexas, J.: Regulation of photosynthesis of C3 plants in response to progressive drought: stomatal conductance as a reference parameter, Ann. Bot., 89, 895–905, https://doi.org/10.1093/aob/mcf079, 2002.

Mehrabi, Z. and Ramankutty, N.: Synchronized failure of global crop production, Nat. Ecol. Evol., 3, 780–786, https://doi.org/10.1038/s41559-019-0862-x, 2019.

Muñoz Sabater, J. 2019. ERA5-Land monthly averaged data from 1950 to present. Climate Data Store (CDS): Copernicus Climate Change Service (C3S)

Peng, Y. and Gitelson, A. A.: Remote estimation of gross primary productivity in soybean and maize based on total crop chlorophyll content, Remote Sens. Environ., 117, 440–448, https://doi.org/10.1016/j.rse.2011.10.021, 2012.

Rathore, L. S., Kumar, M., Moftakhari, H. and Ganguli, P.: Divergent changes in crop yield loss risk due to droughts over time in the US, Environ. Res. Lett., 19, 114008, https://doi.org/10.1088/1748-9326/ad7618, 2024.

Ray, D., Gerber, J., Macdonald, G. and West, P.: Climate variation explains a third of global crop yield variability, Nat. Commun., 6, 9, https://doi.org/10.1038/ncomms6989, 2015.

Satir, O. and Berberoglu, S.: Crop yield prediction under soil salinity using satellite derived vegetation indices, Field Crops Res., 192, 134–143, https://doi.org/10.1016/j.fcr.2016.04.028, 2016.

Schönbeck, L. C., Schuler, P., Lehmann, M. M., Mas, E., Mekarni, L., Pivovaroff, A. L., Turberg, P. and Grossiord, C.: Increasing temperature and vapour pressure deficit lead to hydraulic damages in the absence of soil drought, Plant Cell Environ., 45, 3275–3289, https://doi.org/10.1111/pce.14425, 2022.

https://doi.org/10.5194/egusphere-2026-142
Preprint. Discussion started: 28 January 2026

Tao, F. and Zhang, Z.: Adaptation of maize production to climate change in North China Plain: quantify the relative contributions of adaptation options, Eur. J. Agron., 33, 103–116, https://doi.org/10.1016/j.eja.2010.04.002, 2010.

Tigchelaar, M., Battisti, D. S., Naylor, R. L. and Ray, D. K.: Future warming increases probability of globally synchronized maize production shocks, Proc. Natl. Acad. Sci., 115, 6644–6649, https://doi.org/10.1073/pnas.1718031115, 2018.

Vogel, E., Donat, M. G., Alexander, L. V., Meinshausen, M., Ray, D. K., Karoly, D., Meinshausen, N. and Frieler, K.: The effects of climate extremes on global agricultural yields, Environ. Res. Lett., 14, 054010, https://doi.org/10.1088/1748-9326/ab154b, 2019.

Wang, J., Yan, R., Wu, G., Liu, Y., Wang, M., Zeng, N., Jiang, F., Wang, H., He, W., Wu, M., et al.: Unprecedented decline in photosynthesis caused by summer 2022 record-breaking compound drought-heatwave over Yangtze River Basin, Sci. Bull., 68, 2160–2163, https://doi.org/10.1016/j.scib.2023.08.011, 2023a.

Wang, J., Yang, Y., Huang, J. and Adhikari, B.: Adaptive irrigation measures in response to extreme weather events: empirical evidence from the North China plain, Reg. Envir. Chang., 19, 1009–1022, https://doi.org/10.1007/s10113-018-1442-3, 2019.

Wang, J., Zeng, N., Wang, M., Jiang, F., Chevallier, F., Crowell, S., He, W., Johnson, M., Liu, J., Liu, Z., et al.: Anomalous Net Biome Exchange Over Amazonian Rainforests Induced by the 2015/16 El Nino: Soil Dryness-Shaped Spatial Pattern but Temperature-dominated Total Flux, Geophys. Res. Lett., 50, 11, https://doi.org/10.1029/2023gl103379, 2023b.

Wang, T., Li, N., Li, Y., Lin, H., Yao, N., Chen, X., Li Liu, D., Yu, Q. and Feng, H.: Impact of climate variability on grain yields of spring and summer maize, Comput. Electron. Agric., 199, 16, https://doi.org/10.1016/j.compag.2022.107101, 2022.

Wang, T., Zhang, J., Li, Z., Lin, K., Zhou, W., Wu, G., Pan, M. and Chen, X.: Roles of soil and atmospheric dryness on terrestrial vegetation productivity in China-which dominates at what thresholds, Earth's Future, 13, e2024EF005469, https://doi.org/10.1029/2024EF005469, 2025a.

https://doi.org/10.5194/egusphere-2026-142
Preprint. Discussion started: 28 January 2026

Wang, Y., Shen, Y.-J., Yu, S., Zhang, X. and Xiao, D.: Climate extremes are critical to maize yield and will be severer in North China, Clim. Risk Manag., 100710, https://doi.org/10.1016/j.crm.2025.100710, 2025b.

Wang, Z., Chen, J., Tong, W., Xu, C. and Chen, F.: Impacts of Climate Change and Varietal Replacement on Winter Wheat Phenology in the North China Plain, Int. J. Plant Prod., 12, 251–263, https://doi.org/10.1007/s42106-018-0024-0, 2018.

Wang, Z., Wang, J., Zhou, H., Cai, Q., Yan, R., Wang, H., Huang, Z., Wang, M. and Ju, W.: Loss and recovery of terrestrial carbon sinks induced by 2020 extreme precipitation in the Yangtze River Valley, J. Hydrol., 664, 12, https://doi.org/10.1016/j.jhydrol.2025.134390, 2026.

Wei, Y., Lu, H., Wang, J., Wang, X. and Sun, J.: Dual influence of climate change and anthropogenic activities on the spatiotemporal vegetation dynamics over the Qinghai-Tibetan plateau from 1981 to 2015, Earth's Future, 10, e2021EF002566, https://doi.org/10.1029/2021EF002566, 2022.

Wong, C., Young, D., Latimer, A., Buckley, T. and Magney, T.: Importance of the legacy effect for assessing spatiotemporal correspondence between interannual tree-ring width and remote sensing products in the Sierra Nevada, Remote Sens. Environ., 265, 12, https://doi.org/10.1016/j.rse.2021.112635, 2021.

Xiao, L., Liu, L., Asseng, S., Xia, Y., Tang, L., Liu, B., Cao, W. and Zhu, Y.: Estimating spring frost and its impact on yield across winter wheat in China, Agric. For. Meteorol., 260, 154–164, https://doi.org/10.1016/j.agrformet.2018.06.006, 2018.

Yu, Y., Jinxia, W. and Jikun, H.: The adaptive irrigation behavior of farmers and impacts on yield during extreme drought events in the North China Plain, Resour. Sci., 38, 900–908, https://doi.org/10.18402/resci.2016.05.09, 2016.

Zhang, J., Ge, J., Ma, W., Ding, Z., Wang, X., Li, C., Zhou, B. and Zhao, M.: Research advance on annual water use efficiency of winter wheat-summer maize cropping system in North China Plain, Acta Agron. Sin., 49, 879–892, https://doi.org/10.3724/SP.J.1006.2023.21034, 2023.

Zhang, Q., Cheng, Y., Lyapustin, A., Wang, Y., Gao, F., Suyker, A., Verma, S. and Middleton, E.: Estimation of crop gross primary production (GPP): fAPARchl versus MOD15A2 FPAR, Remote Sens. Environ., 153, 1–6, https://doi.org/10.1016/j.rse.2014.07.012, 2014.

https://doi.org/10.5194/egusphere-2026-142
Preprint. Discussion started: 28 January 2026

Zhang, W., Zhou, T., Ye, W., Zhang, T., Zhang, L., Wolski, P., Risbey, J., Wang, Z., Min, S.-K. and Ramsay, H.: A Year Marked by Extreme Precipitation and Floods: Weather and Climate Extremes in 2024, Adv. Atmos. Sci., 42, 1045–1063, https://doi.org/10.1007/s00376-025-4540-4, 2025.

Zhao, Z., Qin, X., Wang, Z. and Wang, E.: Performance of different cropping systems across precipitation gradient in North China Plain, Agric. For. Meteorol., 259, 162–172, https://doi.org/10.1016/j.agrformet.2018.04.019, 2018.

Zhou, X., Geng, X., Yin, G., Hänninen, H., Hao, F., Zhang, X. and Fu, Y. H.: Legacy effect of spring phenology on vegetation growth in temperate China, Agric. For. Meteorol., 281, 107845, https://doi.org/10.1016/j.agrformet.2019.107845, 2020.